Development of a Steering Angle and Torque Sensor of Contact-type

*by Akira Noguchi *, Kosuke Yamawaki *, Toshiro Yamamoto *2 and Tomoaki Toratani *2*

ABSTRACT With the growing concern over the global environment in recent years, environmental preservation technologies are required to be developed in the field of automotive industries also. Accordingly, there is an increasing need for electric power steering system (EPS) of low energy consumption to replace hydraulic power steering system conventionally used. Because steering angle and torque sensors used in the EPS are based on contact-type sensing, they tend to have such problems as delayed response caused by the friction of the sensing brush against conductive resin in addition to friction noise. The authors have developed, by studying structures of the rotor and the sliding portions, a low friction noise sensor with outstanding electrical performance.

1. INTRODUCTION

In modern automobiles in which comfortability and safety of steering are highly required, power steering system has become an essential component enabling adjustment of steering assisting force whenever needed during stop time and low- or high-speed driving. The hydraulic power steering system conventionally used for steering control consumes, since a hydraulic pump has to be driven full-time, 4～5 HP constantly, which corresponds to a loss of about 3 % in terms of fuel consumption. The electric power steering system (EPS), in contrast, consumes less energy since its assist motor is driven at the time of steering operation only, and also has an advantage of space saving due to its simplified structure. Thus the demand for this system is expected to rapidly grow in future.

In EPS a steering angle and torque sensor is needed, which detects rotation torques applied on the torsion bar of the steering shaft together with steering angles (rotation angle) at the time of steering, and subsequently inputs these torque and angle signals, in order to determine the control output, into electronic control unit (ECU) that controls the rotation force of the assist motor. The steering angle and torque sensor reported here has been designed and developed against this background.

2. REQUIRED SPECIFICATIONS

Figures 1 and 2 show the mechanism for torque and angle sensing of the sensor developed here. A torque-sensing pattern is printed on one side of the resistive element substrate that rotates combined with the column-side rotor, and an angle-sensing pattern is printed on the other side. The torque-sensing side is in contact with and slides on brushes provided on the steering-

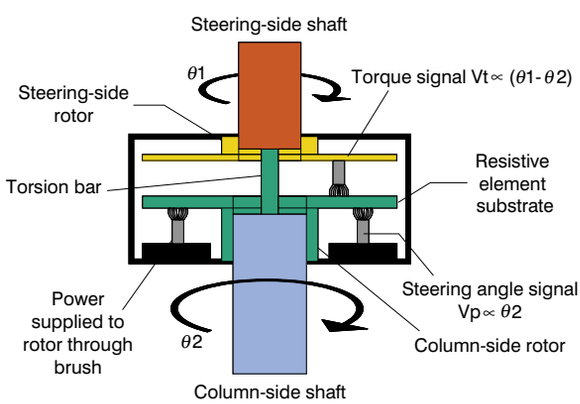

Figure 1 Torque and angle sensing mechanism (Ⅰ).

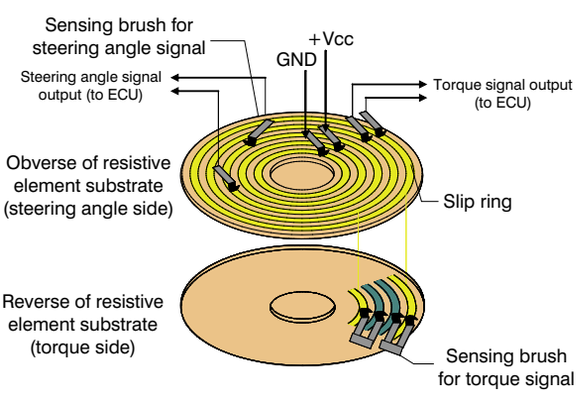

Figure 2 Torque and angle sensing mechanism (Ⅱ).

* Engineering Dept., Automotive Products Div.
*2 Advanced Production Systems Center, Plant and Facilities Div.

side rotor, while the steering-angle side is in contact with other brushes provided on the output substrate in the sensor housing. Thus the contact positions of the brushes with the substrates change according to the twist of torsion bar and the rotation of steering wheel during car driving, so that torque and angle signals are output in conformity with the required specifications. Indispensable performance for this sensor includes:

1) Steerability: To supply signal outputs of fast response and high accuracy so as to offer a comfortable steering feeling during car driving.
2) Durability: To supply noiseless output signals over several hundreds thousands of kilometers of distance driven.
3) Quietness: To reduce friction noise generated by the sensor.

This report describes the development as well as the improvement of steerability and quietness.

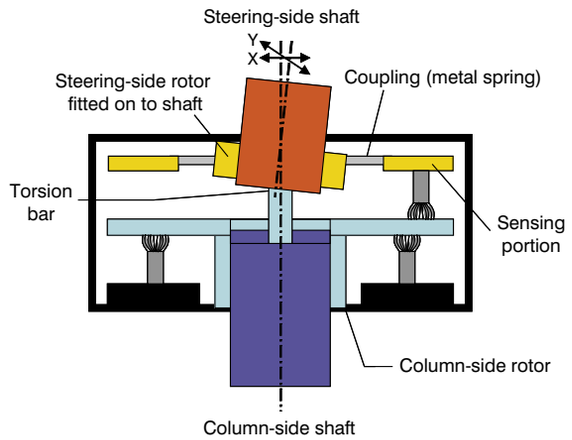

Figure 3 Coupling structure connecting the sensing portion with the shaft.

3. SOLUTIONS TO THE REQUIRED SPECIFICATIONS AND THE RESULTS

3.1 Steerability

3.1.1 Objectives in Steerability Improvement

Because in EPS the steering assisting force is adjusted based on the output signals from its sensor, the sensing function of an EPS sensor is very influential over the entire system. If the sensor has poor responsiveness of output signals to shaft rotation and oscillation during car driving, the smoothness of steering feeling will be lost sometimes resulting in a scratchy feeling of steering. The responsiveness of output signals depends on the tracking performance of the sensing brushes that slide, as the shaft rotates and the torsion bar twists according to steering, on the slip rings of the rotating substrate. The responsiveness tends to deteriorate as the frequency of steering shaft oscillation increases, making it an essential task for development how to maintain the signal response fast at high frequencies whereby the shaft rotates. Factors in degradation of signal response include:

1) Backlash in the shaft bearing portion comprising a number of constituting parts
2) Sliding friction at the bearing portions for the steering-side rotor and for the column-side rotor
3) Inertia due to rotation
4) Deteriorated stiffness of constituting parts such as the steering-side rotor

Based on these standpoints, we proceeded to fabricate prototypes and evaluate their performance so as to optimize the design.

3.1.2 Measures for Improving Signal Responsiveness

If the backlash and the sliding friction mentioned above could be eliminated, signal delay might not be generated. However, it is impossible to completely remove these degradation factors since both the sensor and the steering shaft are mechanical elements. In practice, signal responsiveness of the sensor itself was improved to a certain degree by countermeasures such that the backlash in the shaft bearing portion is reduced as much as possible by fine tuning the molding dies to improve the dimensional accuracy and tolerance of constituting parts, and friction is decreased by finely polishing the molding dies for the bearing portion to minimize the sliding surface roughness of the bearing portion.

The inertia due to rotation was dealt with by reducing the weight and volume of the steering-side rotor as much as possible, but we had to be satisfied with a certain degree of reduction.

With respect to the stiffness degradation of constituting parts, the signal responsiveness would significantly improve if all the structures from the fitting portion of the steering-side shaft to the actual sensing portion were connected using a rigid body without elasticity. In the shaft structure shown in Figure 1, however, axial and angular misalignment in the X-Y plane readily occurs between the steering-side and column-side shafts, so that, if the steering-side rotor is composed of a rigid body and axial misalignment occurs between the shafts, a significant load will be imposed on the bearing portion of the sensor, thereby increasing the sliding friction and adversely affecting the durability of the bearing portion.

We have decided, therefore, to set up a coupling of metal spring between the rotor fitted on the shaft and the sensing portion, as shown in Figure 3. Although the coupling was intended to absorb the possible eccentricity of the shaft in the X-Y plane so as not to increase the sliding friction, it was found that the result of an experiment was unsatisfactory, in which a prototype using this coupling structure was fabricated and integrated with the shaft to confirm the signal responsiveness. Accordingly, we immediately investigated the matter to take measures.

3.1.3 Design of Steering-side Rotor with Coupling

There were two factors to be considered in designing the optimized structure of the steering-side rotor to meet the requirements for signal responsiveness from the standpoint of stiffness. One is to make allowance for

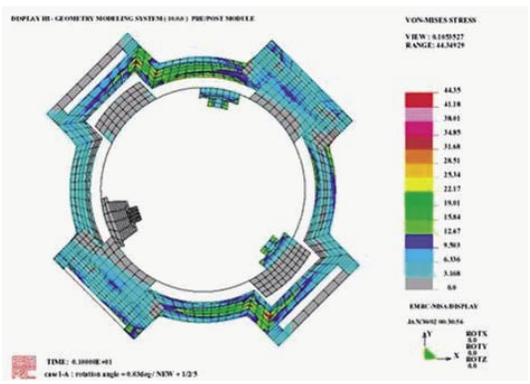

Figure 4 Result of FEM analysis.

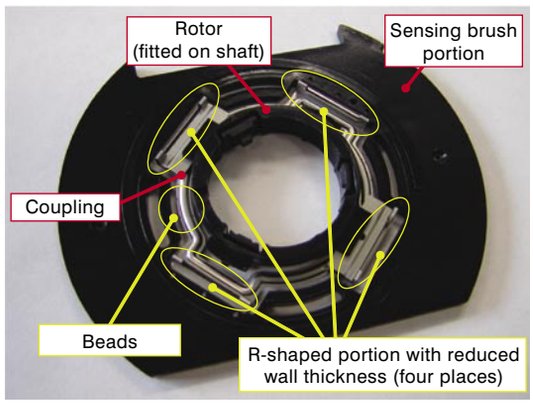

Photo 1 Steering-side rotor after design change.

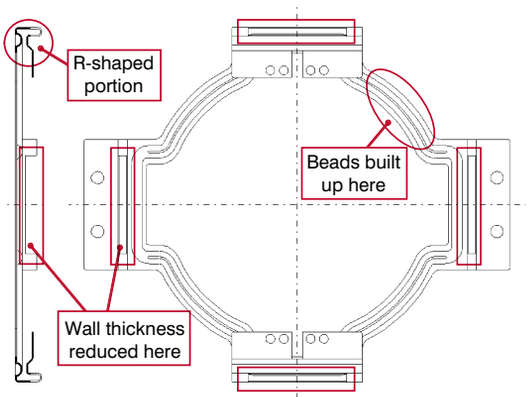

Figure 5 Design changes of coupling.

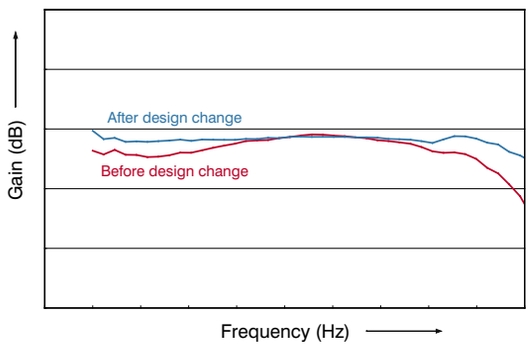

Figure 6 Comparison of the frequency characteristics of signal amplitude before and after design changes.

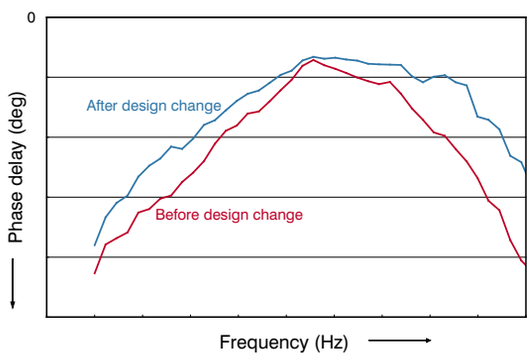

Figure 7 Comparison of the frequency characteristics of signal phase delay before and after design changes.

flexures of the steering-side and column-side shafts in the X-Y plane in order to absorb the axial misalignment of these shafts. The other is to provide the rotor with sufficient stiffness in the direction of rotation to prevent delayed response.

Accordingly finite element method (FEM) analysis was carried out in terms of strain and stress to obtain the optimized sensor configuration that could remove these two factors simultaneously. After setting up material properties and sensor configurations, torque and stress applied on the steering-side rotor from the shaft were input to analyze the stress and strain over the entire rotor, and subsequently investigations were made based on the result of the analysis to find out suitable changes of the current design.

Figure 4 shows the result of an FEM analysis, and Figure 5 and Photo 1 illustrate the design changes in the coupling structures effected based on this analysis. With respect to the flexure in the X-Y plane, the wall thickness of the R-shaped portion was greatly reduced to permit flexures of this portion. As a result, it was proved that this structure could absorb the backlash, suppressing the growth of sliding friction between the parts in case of occurrence of eccentricity between the two shafts.

On the other hand, beads were built up to increase the stiffness of the entire coupling in the direction of rotation, and the wall thickness of the coupling as well as the related rotor was increased reviewing the design of the entire steering-side rotor, and the result was that the shaft rotation tracking performance of the brush provided at the sensing portion was much improved. Thus even when high frequency oscillation was imposed on the shafts, the signal responsiveness was seen to be enhanced. Figures 6 and 7 show the improvements in signal responsiveness in terms of amplitude and phase versus rotation frequency at the time of shaft oscillation.

Moreover, prototypes of the modified sensor were installed on a test car to verify the steering feeling. The experimental results confirmed that the prototype gave no scratchy feeling during steering rotation, satisfactorily meeting the requirement for steerability.

3.2 Quietness

3.2.1 Objectives in Quietness Improvement

Recently, car manufacturers are emphasizing quietness improvement of vehicles as a whole, so that requirements for individual parts constituting a vehicle are growing in severity. With regard to the steering angle and torque sensor of contact-type also, reduction of the noise generated by the sensor was stringently required from the beginning of development. In particular the peak sound pressure at 3150 Hz, specified by JIS C 1513 as a center frequency with third-octave-band, had been considered problematic, necessitating an immediate investigation.

Noise generated by the sensor include the sliding noise of the contact point between the brushes and the substrate at the time of steering rotation and that between plastic housings for the bearing portion of the sensor. Specifically the noise between the brushes and the substrate sounds very stridently since both of the two surfaces are metallic. Accordingly investigation was focused on identifying the cause of, and devising a countermeasure against, the noise between the brushes and the substrate, under the suspicion that the peak sound pressure at 3150 Hz mentioned above coincided with this noise.

3.2.2 Brush Design Aimed at Sliding Noise Reduction

Design of the brush was investigated first.

In the first place, in order to measure the natural frequency of the brush sliding over the substrate while the steering shaft rotates, an experimental sensor was fabricated which permits external observation of a brush in contact with a substrate, and vibration frequency of the brush during sensor rotation was measured using a laser vibrograph. The schematic of the measurement is shown in Figure 8.

As a result, it was confirmed that all the brushes to be installed had a natural frequency very close to 3150 Hz.

Simultaneously with this, FEM analysis was performed to verify several vibration modes that are likely to appear during brush sliding. Figure 9 shows a vibration mode that is most likely to appear. It corresponds to one of the lateral vibration modes of the contact wire, which is provided on the tip of the brush to constitute an actual sliding interface, while the wire slides over the substrate surface, and its frequency of 3157 Hz is very close to the frequency of 3150 Hz above mentioned. Whereas vibration of the brush arm with large amplitudes was not

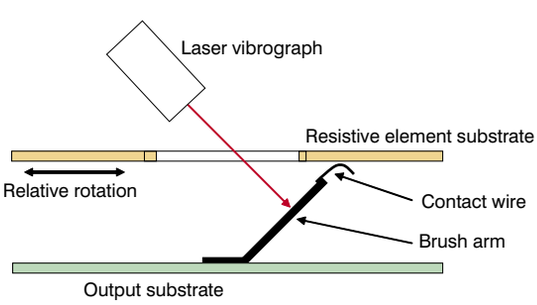

Figure 8 Schematic of vibration measurement for brush.

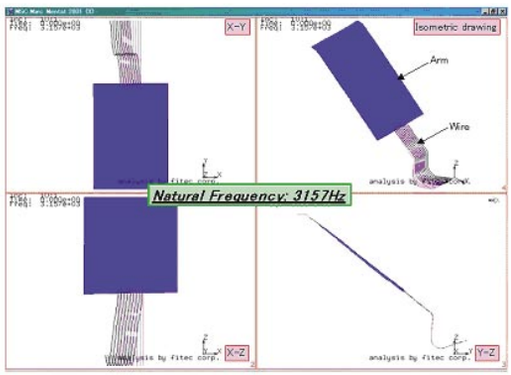

Figure 9 Vibration mode of sliding brush (by FEM analysis).

observed in this mode, other modes were confirmed in which the brush vibrates vertically.

It was thus confirmed from the results and analysis of vibration mentioned above, that the sound in question at 3150 Hz is generated by the following mechanism:

- The contact wire on the brush tip vibrates reciprocally, while it slides over the substrate surface, in the direction lateral to the wire length.
- This vibration propagates to the brush arm, making the wire and the brush arm as a whole vibrate at 3150 Hz.
- The brush arm amplifies the vibration to generate a high-pitched sound.

Based on this result of verification, we proceeded to develop countermeasures against noise that are realizable in consideration of mass production.

3.2.3 Substrate Plating Aimed at Sliding Noise Reduction

Verification of substrate design was performed in parallel with the verification of the brush design.

In addition to the fact that a peak sound pressure was generated at 3150 Hz due to the sliding action of the brush installed on the output substrate over the surface of the resistive element substrate, it was found that variations of plating conditions of the substrate surface existed between the lots, resulting in a sound pressure difference of as much as 10 dB depending on the lot. Accordingly comparisons in terms of plating compositions and plating conditions were made to verify the differences between the substrates with high sound pressure and those with low sound pressure.

Photos 2 and 3 show the plated surface conditions of high sound pressure and those of low sound pressure, respectively. It could be confirmed that while the sample of high sound pressure shown in Photo 2 had a rough surface, that of low sound pressure shown in Photo 3 had a finely plated surface. An attempt was made, therefore, to correlate the averaged surface roughness (R_a) or the maximum surface roughness (R_{max}) with the sound pressure, but this idea was soon abandoned because no correlation was found. In an effort to find out a suitable indicator that is correlated with the sound pressure, we paid attention to the sliding friction force with the brush.

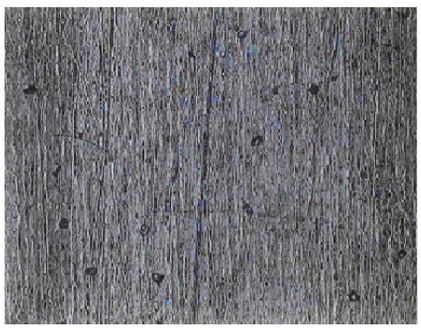

Photo 2 Plated surface of high sound pressure substrate (× 250).

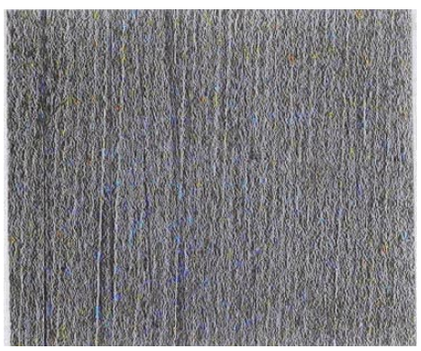

Photo 3 Plated surface of low sound pressure substrate (× 250).

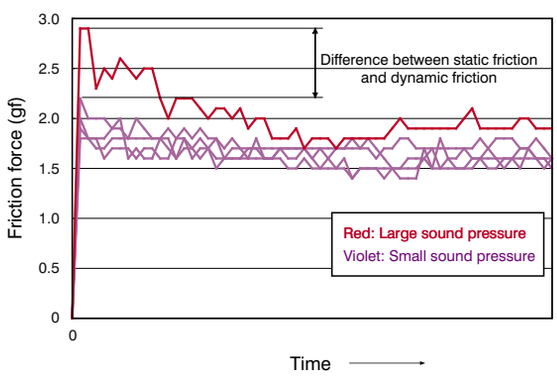

Figure 10 Measurement results of friction forces between plated surface and brush.

The friction force between the brush and the plated surface of the resistive element substrate was measured using an exclusive instrument incorporating a force gauge with a turntable, and the results are shown in Figure 10. It was shown that the plated surface with low sound pressure had a low sliding friction force with the brush, so that we proceeded to investigate surface treatment methods for low sliding friction force to achieve sound pressure reduction.

3.2.4 Implementation of Countermeasures

We have investigated countermeasures against the sound pressure peak at 3150 Hz based on the verification of brush design and plated surface treatment, and decided to take the countermeasures described below.

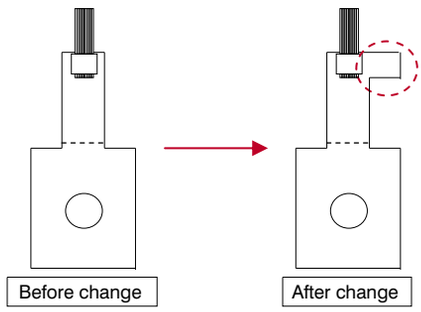

Figure 11 Design change of brush.

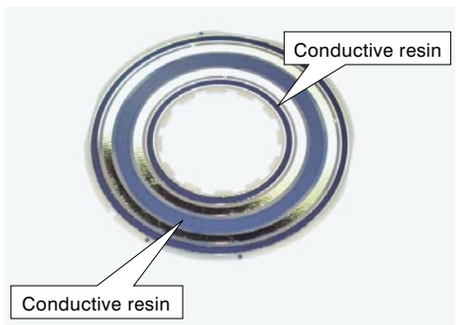

Photo 4 Resistive element substrate coated with conductive resin.

Firstly, based on the verification of the brush design, changing the configurations of the contact wire and the brush arm was studied, and it became clear that increasing the mass of the brush was most effective, and this was included as one of the design changes. Figure 11 shows changes in the brush configuration. In view of the mounting space for the brush in addition to maintaining the proven reliability of brush contact, an increment of the brush weight was given by making the brush arm configuration asymmetry.

What is more, to improve the surface treatment for reduction of the sliding friction of the brush, the plated surface was coated with conductive resin, and the treatment method for the plated surface was changed. As shown in Photo 4, coating the resistive element substrate with conductive resin can make the sliding surface smooth because, even if the plated surface should be rough, the resin will permeate the surface. Moreover, for plated surfaces where resin coating is not very effective, a new plating method for low friction was adopted, whereby chemical polishing treatment was carried out thoroughly as a pre-process of the Ni and Au plating. This enabled suppression of variations in surface roughness and surface irregularities, resulting in the smooth surface of plating as shown in Photo 5.

These measures brought about a considerable reduction of the peak sound pressure of significant magnitude at 3150 Hz. Figure 12 shows the results of third-octave-band frequency measurements before and after the implementation of these measures.

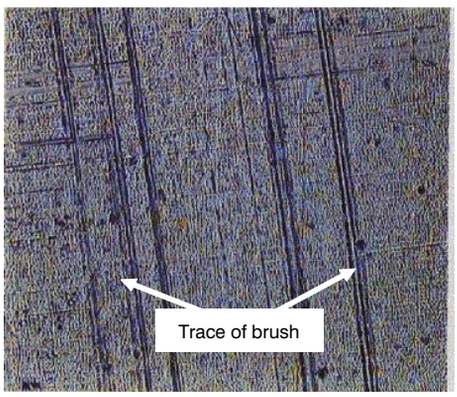

Photo 5 Au plated surface of substrate after countermeasure implementation (× 250).

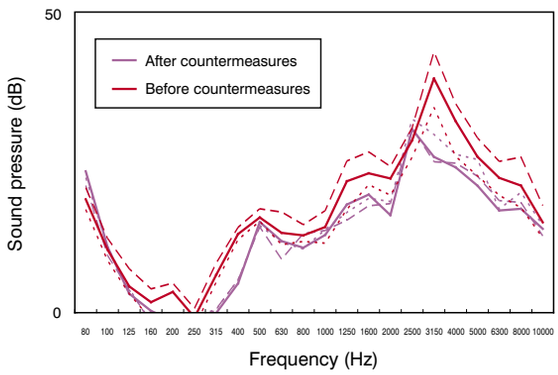

Figure 12 Sliding friction noise of substrates before and after countermeasure implementation.

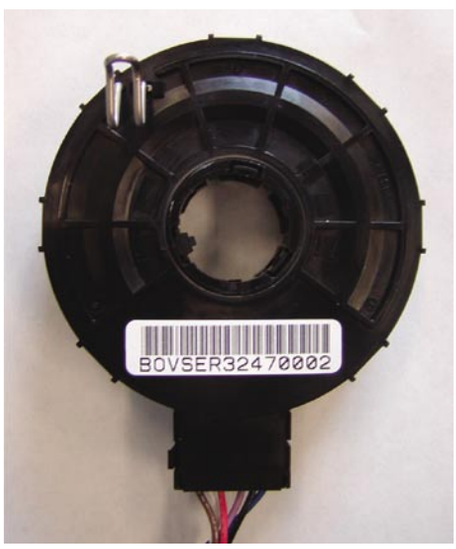

Photo 6 Appearance of steering torque and angle sensor.

4. FUTURE DEVELOPMENT

The sensor developed here has achieved the improvements in terms of steerability, durability and quietness as were required by our customers, and has been in mass production since April, 2003. Photo 6 shows an appearance of the sensor. In the future, we plan to reduce the cost as well as to improve its steerability and quietness further.

5. CONCLUSION

In the development of this steering angle and torque sensor of contact-type, which was required to provide higher performance than conventional sensors, we have been successful in overcoming many problems and in launching into mass production through the concentration of efforts of people involved. In view of the increasing demand for EPS that is predicted, the demand for this sensor is expected to grow also.

We would like to express our sincere gratitude to Tokyo Cosmos Electric Co., Ltd. and concerned parties for their cooperation in developing this sensor.